AD-A039 706 COLORADO STATE UNIV FORT COLLINS DEPT OF CHEMISTRY F/G 20/2
RAMAN SPECTRA OF SIF4 AND GEF4 CRYSTALS.(U)
APR 77 E R BERNSTEIN, G R MEREDITH N00014-75-C-1179
UNCLASSIFIED TR-11 NL

| OF |
AD
A039706

END

DATE
FILMED
6-77

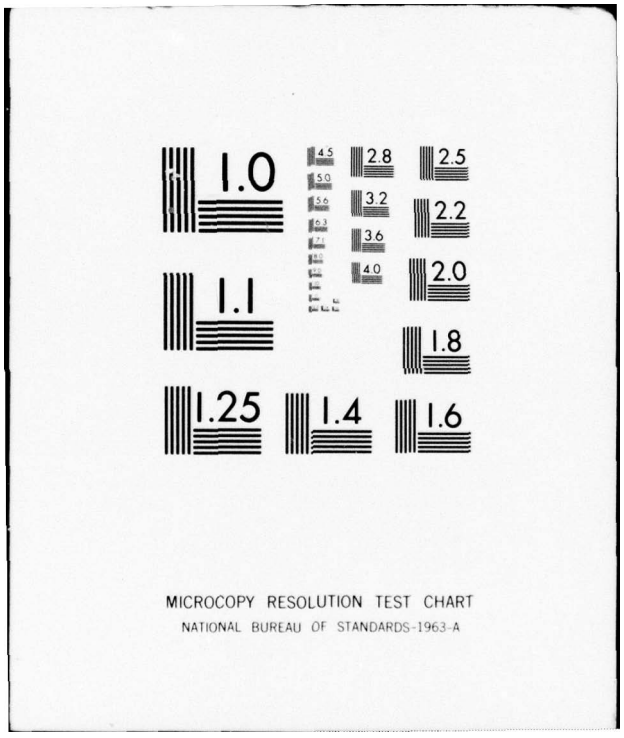
1.0
1.1
1.25
1.4
1.6
1.8
2.0
2.2
2.5
2.8
3.2
3.6
4.0
4.5
5.0
5.6
6.3
7.1
8.0
9.0
MICROCOPY RESOLUTION TEST CHART
NATIONAL BUREAU OF STANDARDS-1963-A

OFFICE OF NAVAL RESEARCH

Contract N00014-75-C-1179

Task No. NR 056-607

TECHNICAL REPORT NO. 11

"Raman Spectra of SiF_4 and GeF_4 Crystals"

by

E. R. Bernstein and G. R. Meredith*

Prepared for Publication
in the
Journal of Chemical Physics

Department of Chemistry
Colorado State University
Fort Collins, Colorado 80523

April 1977

*Current address: Department of Chemistry
University of Pennsylvania
Philadelphia, PA 19174

UNCLASSIFIED
SECURITY CLASSIFICATION OF THIS PAGE (When Data Entered)

REPORT DOCUMENTATION PAGE

READ INSTRUCTIONS BEFORE COMPLETING FORM

1. REPORT NUMBER: (14) TR - 11
2. GOVT ACCESSION NO.:
3. RECIPIENT'S CATALOG NUMBER:
4. TITLE (and Subtitle): (6) Raman Spectra of SiF_4 and GeF_4 Crystals.
5. TYPE OF REPORT & PERIOD COVERED: (9) Technical Report.
6. PERFORMING ORG. REPORT NUMBER:
7. AUTHOR(s): (10) E. R. Bernstein and G. R. Meredith
8. CONTRACT OR GRANT NUMBER(s): (15) N000014-75-C-1179
9. PERFORMING ORGANIZATION NAME AND ADDRESS: Colorado State University, Dept. of Chemistry, Fort Collins, CO 80523
10. PROGRAM ELEMENT, PROJECT, TASK AREA & WORK UNIT NUMBERS: NR 056-607
11. CONTROLLING OFFICE NAME AND ADDRESS: Office of Naval Research, Arlington, VA 22217
12. REPORT DATE: (11) April 1977
13. NUMBER OF PAGES: 45
14. MONITORING AGENCY NAME & ADDRESS (if different from Controlling Office): (12) 44p.
15. SECURITY CLASS. (of this report): Unclassified
15a. DECLASSIFICATION/DOWNGRADING SCHEDULE:
16. DISTRIBUTION STATEMENT (of this Report): Approved for public release, distribution unlimited.

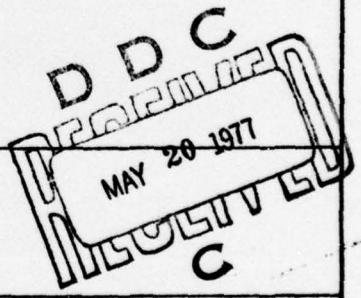

17. DISTRIBUTION STATEMENT (of the abstract entered in Block 20, if different from Report):
18. SUPPLEMENTARY NOTES:
19. KEY WORDS (Continue on reverse side if necessary and identify by block number):

Raman spectra
molecular crystals
polaritons
exciton states

20. ABSTRACT (Continue on reverse side if necessary and identify by block number):

The Raman scattering spectra of large single crystals of SiF_4 and GeF_4 at 77K are reported. These data have been reinterpreted based on the absence of any observable changes in the spectra for scattering angles between 0° and 90°. The previous assignment of the dipole allowed (ν_3) and

DD FORM 1 JAN 73 1473 EDITION OF 1 NOV 65 IS OBSOLETE
S/N 0102-014-6601

UNCLASSIFIED
SECURITY CLASSIFICATION OF THIS PAGE (When Data Entered)

404 992 LB

20.

ν_4 modes in terms of a TO/LO splitting (i.e., polariton) model is thereby shown to be incorrect. In the absence of an apparently correct crystal structure, an exact interpretation of the data in terms of a factor group-exciton analysis is not possible; nonetheless all observations are shown to be consistent with a multimolecular primitive (non-cubic) unit cell. Mixed SiF_4/GeF_4 crystal spectra have also been obtained which demonstrate that GeF_4 does not substitute into the SiF_4 lattice but that SiF_4 does enter the GeF_4 crystal substitutionally.

Abstract

The Raman scattering spectra of large single crystals of SiF_4 and GeF_4 at 77K are reported. These data have been reinterpreted based on the absence of any observable changes in the spectra for scattering angles between 0° and 90°. The previous assignment of the dipole allowed ν_3 and ν_4 modes in terms of a TO/LO splitting (i.e., polariton) model is thereby shown to be incorrect. In the absence of an apparently correct crystal structure, an exact interpretation of the data in terms of a factor group-exciton analysis is not possible; nonetheless all observations are shown to be consistent with a multimolecular primitive (non-cubic) unit cell. Mixed SiF_4/GeF_4 crystal spectra have also been obtained which demonstrate that GeF_4 does not substitute into the SiF_4 lattice but that SiF_4 does enter the GeF_4 crystal substitutionally.

I. INTRODUCTION

Inorganic volatile fluorides are excellent systems for study of the finer details of molecular crystal phenomena: their molecular spectra are generally simple due to the high symmetry and small number of atoms, and there is generally more than one member of a chemical series. In this paper the (internal) vibrational properties of SiF_4 and GeF_4 crystals will be discussed.[1-9]

There have been numerous previous studies of the vibrational spectra of polycrystalline SiF_4 and these are reviewed in the following section. No reports of the crystal vibrational spectra of GeF_4 have appeared. Our interest in the Raman scattering of single crystal GeF_4 and SiF_4 was attracted by the reported large transverse optical (TO)-longitudinal optical (LO) splitting for the dipole allowed ν_3 and ν_4 modes of SiF_4 [$\delta(\nu_3)$ ~70 cm^{-1} and $\delta(\nu_4)$ ~30 cm^{-1}]. Such large splittings in cubic crystals should give rise to substantial <u>polariton</u> effects which, for molecular solids, seemed unlikely to us. Comparison with other dipole-allowed organic and inorganic molecular crystal vibrational exciton transitions (C_6H_6, MF_6) confirmed this suspicion. Indeed, the new data presented here for 0° and 90° Raman scattering do not support these assignments, as the scattering mode intensity and energy are scattering angle independent. The spectra are consequently reinterpreted in the more usual molecular crystal fashion in terms of exciton splittings of molecular levels arising from a crystal with more than one molecular per primitive unit cell. The major stumbling block to a complete crystal spectra assignment is an incorrectly determined crystal structure.

The general concepts of polaritons as phonon-photon coupled polarization modes in non-centrosymmetric crystals[10-23] are reviewed in Section III.

II. REVIEW OF PREVIOUS STUDIES

Both SiF_4 and GeF_4 are gases at room temperature and their infrared and Raman spectra have been studied and interpreted.[1] The four vibrations of an XY_4 T_d molecule, ν_1 through ν_4, transform as a_1, e, t_2, and t_2 respectively.

The crystal structure of SiF_4 was determined[2] at -145°C via X-ray diffraction to belong to the space group T_d^3. This is a body centered cubic structure with one molecule per primitive unit cell at a T_d site. The only solid-solid phase transition known[3] is a first order transition observed at 8.2×10^3 kg/cm^2 and 175 K. Heat capacity measurements down to 15 K have revealed no transitions at normal pressures.[4]

The vibrational spectra of SiF_4 crystals first appeared in connection with a discussion of dipole summations.[5] Whenever a transition is dipole allowed, the $\underline{k} \neq 0$ crystal levels should exhibit TO/LO splitting and therefore polariton behavior. In addition to such apparent splittings, however, a further splitting was noted for the low energy ν_3 component. If the polariton assignment is then still accepted, the TO mode degeneracy is removed, requiring a different crystal structure. An alternative crystal structure was proposed, O_h^9 with eight molecules per primitive unit cell, which is entirely too complex to fit the relatively simple infrared and Raman spectra. (Consider also the lack of infrared/Raman mutual exclusion which is predicted for O_h^9 structures.) Fox and Hexter[6] later suggested that the low energy ν_3 component splitting is a consequence of crystal size and shape (boundary conditions on the slowly converging dipole summations). Bessette et al.,[7] however, showed that the splitting was preserved even for "large" crystals grown from the melt. Additionally they observed ν_1 in infrared absorption. Coupling this fact with constancy

of the spectra as temperature was varied, they concluded that the crystal structure was indeed in error. They suggested C_3^4 or C_{3v}^5 space groups to describe structures differing from the T_d^3 structure by only small deviations. They agree that the large splitting of the ν_3 and ν_4 modes should be assigned to TO/LO structure. They base their conclusion on the following observations: 1) the higher energy component is much more intense in the Raman spectra (the LO peak is disallowed in cubic crystals' infrared absorption spectra, but observed due to beam convergence); 2) the strong infrared reflection band is bracketed by the TO and LO energies; 3) approximate agreement of calculated TO/LO splittings for the ν_3 and ν_4 bands (based on vapor phase oscillator strengths) with the observed splittings; and 4) lineshapes for ν_3 and ν_4 in liquid Raman spectra are asymmetric with widths comparable to the TO/LO splittings observed in crystals.

The remaining crystal investigations deal with the observation of two-particle bands (which have only been observed in infrared absorption). The marked similarity of $\nu_1 + \nu_3$, $\nu_1 + \nu_4$, and $\nu_2 + \nu_3$ bands is considered strong support for the dipolar nature of the interactions.[8] Calculated $2\ \nu_3$ two-phonon band structure is in reasonable agreement with experiment.[9] In these studies the T_d^3 crystal structure was assumed.

III. THEORY

The theory of energy levels and first order Raman processes in crystals has been discussed extensively.[10] Briefly, we will review the pertinent features necessary to follow our basic reasoning and logic.

For crystals with inversion centers, factor group analysis ($\underline{k} = 0$ exciton predictions) will explain the first order Raman spectra since the dispersion ($dE/d\underline{k}$) is very small over the range of optically accessible wavevectors. On the other hand, for crystals without inversion centers, those levels which are dipole allowed may interact with the electromagnetic field in such a way that a very rapid dispersion behavior is predicted near $\underline{k} = 0$. This variation of energy with crystal wavevector (for $\underline{k}$ order of the wavevector of light), is accessible by Raman spectroscopy.[11-14] For vibrational levels there result various separations of modes (at small $\underline{k}$) which are predicted to be degenerate by factor group analysis (at $\underline{k} = 0$). These separations are essentially constant at wavevectors characteristic of visible light, but may vary with the orientation of the wavevector in the crystal. Of course at strictly $\underline{k} = 0$ the appropriate factor group analysis obtains, $\underline{k} = 0$ level structure may not, however, be accessible to optical measurements.

For SiF_4 (or GeF_4) cubic crystals (T_d^3) the t_2 molecular vibrations are unsplit by mechanical interactions. The coupling with the electromagnetic field is described by the dispersion relation[11-14]

$$\omega = kc/[\epsilon(\omega)]^{1/2} = kc/\left[\epsilon_\infty + \sum_j \frac{|\underline{E}_e|}{|\underline{E}|} \frac{4\pi A \left(\frac{\partial \mu}{\partial Q_j}\right)^2}{\omega_j^2 - \omega^2 - i\omega\gamma_j}\right]^{1/2} \qquad (1)$$

in which $k = 2\pi/\lambda$, $\omega = 2\pi\nu$, λ is the wavelength of the periodic excitation of frequency ν, A is the number of molecules per unit volume, $|\underline{E}_e| / |\underline{E}|$ is a local field correction ($[(\epsilon_\infty + 2)/3]^2$) for sites of tetrahedral or higher

symmetry), ϵ_∞ is the infinite (optical) frequency dielectric constant, ω_j is the angular frequency of the jth TO mode with dipole derivate $\left(\frac{\partial \mu}{\partial Q_j}\right)$, and γ_j is a dampling constant for that mode. We will ignore effects of the damping constants. TO and LO modes are those for which equation 1 is satisfied as $\epsilon(\omega) \to \infty$ and $\epsilon(\omega) \to 0$, respectively. With more than one mode j, the Lyddane-Sachs-Teller relationship must be generalized to

$$\prod_j \left(\frac{\omega_{Lj}}{\omega_j}\right)^2 = \frac{\epsilon_o}{\epsilon_\infty} \tag{2}$$

in which ω_{Lj} is the LO frequency of the jth mode. Examples of the dispersion relationship of equation 1 for two-coupled vibrational modes may be seen in Figure 1 for $k \sim 0$.

One might be interested also in the relationship of ω_j to ω_{oj}, the mechanically determined (in the absence of the radiation field) vibrational frequency.[14] For a separated band

$$\omega_j^2 = \omega_{oj}^2 - \frac{|\underline{E}_e|}{|\underline{E}|} \frac{4\pi A}{3} \left(\frac{\partial \mu}{\partial Q_j}\right)^2 . \tag{3}$$

However, this number is not useful to us since the mixed crystals under investigation will be subject in principle to strong polarization of the host (induced dipoles) by the vibrating guest. The apparent site energies will be reduced from ω_o. This problem is beyond the scope of the current study.

For vibrational Raman scattering with visible or ultraviolet light, the phonon energy is small compared to photon energies so that the incoming and scattered photons have approximately equal magnitude wavevectors. For scattering at some angle θ (Figure 2) wavevector conservation requires

$$\underline{k} = \underline{k}_i - \underline{k}_s . \tag{4}$$

For arbitrary Θ

$$|\underline{k}| = \left[\frac{\omega^2 \epsilon_\infty}{c^2} + 4|\underline{k}_i|\left(|\underline{k}_i| - \frac{\omega \epsilon_\infty^{1/2}}{c}\right)\sin^2(\Theta/2)\right]^{1/2}. \qquad (5)$$

By varying Θ , $|k|$ can be made small. These phase matching conditions appropriate to Raman scattering with the 5145Å Ar^+ laser line are drawn in Figure 1 for various scattering angles. To generate these curves, a value of the dielectric constant which relates the vacuum wavevector (wavenumber) to $|\underline{k}_i|$ in the crystal is required. In equation 1 ϵ_∞ indicates the background (electronic) dielectric constant in the low frequency (infrared) region. In the visible region ϵ_∞ will generally have a larger value. The effect of this dispersion is to tilt the phase matching curves at higher ν towards larger $|\underline{k}|$. This effect is not expected to be important for our conclusions.

For uniaxial crystals the dispersion relation is not as simple as equation 1. The orientation of $\underline{k}$ relative to the $\hat{c}$ (optic) axis becomes important since the mechanical vibrations are no longer degenerate. Loudon[11] has discussed this effect and we merely present representative dispersion curves in Figure 3. He has in addition presented scattering efficiencies by polariton and longitudinal modes as functions of Θ . His expressions are not applicable for small angles since he has neglected the $\frac{\omega \epsilon_\infty^{1/2}}{c}$ terms in equation 5.

Generally for regions in which the excitation is largely photon-like, a three wave mixing mechanism will induce transitions while in the phonon-like regions a vibrational Raman mechanism will be dominant. In intermediate regions a mixture of these will occur with the possibility of interference effects. Of course both tensors involved will have the same transformation properties so one need only consider the Raman tensor.

Selection rules for TO-polariton and LO modes in cubic (T_d) crystals have been discussed[15,21-23] as a function of scattering angle and crystal

momentum direction. Both modes are allowed for general wavevector directions. In certain restrictive instances (i.e., T_d structure $\underline{k}_i || (100)$) for forward scattering ($\Theta = 0$), only LO modes are predicted. However, in cases for which $\Theta \neq 0$ the angle of $\underline{k}$ relative to $\underline{k}_i$ (ϕ) is given by

$$\sin(\phi) = (|\underline{k}_i| - \omega \epsilon_\infty^{1/2}/c) \sin(\Theta)/|\underline{k}|. \tag{6}$$

Equation (6) emphasizes that for Θ small but nonzero, (the experimental situation at hand) ϕ is not close to 0° or 90° (see Figure 2) so that both LO and TO modes become allowed. Therefore we conclude that, even in the most ideal case for SiF_4 and GeF_4 (T_d^3 space group), both components should be experimentally accessible, irrespective of $\underline{k}_i$ direction in the crystal. The intensity of given LO and TO modes, of course, will in general be a sensitive function of scattering angle for Θ <10°.

IV. EXPERIMENTAL

Large (~6 x 6 x 20 mm) single crystals of SiF_4, GeF_4, 5% SiF_4 in GeF_4 and 5% GeF_4 in SiF_4 were prepared for 90° scattering measurements. Details of the syntheses and crystal techniques are available in reference 16. A 25 mm diameter by 2 mm thick disc of SiF_4 was grown in polished quartz cell for small angle scattering experiments. All spectra were obtained at liquid nitrogen temperature utilizing the 5145Å line of an Ar^+ laser. Details of the Raman apparatus and experimental precautions may also be found in reference 16. To obtain accurate 0° scattering data the optics were limited in aperature to roughly f/100; this gives an angular acceptance of roughly 0.5° for the unfocused TEM_{oo} laser beam.

Over 600 Fe-Ne hollow cathode lamp lines were fitted to a calibration curve which included a term to correct for the small cam action of the screw of the monochromator. Each measurement had a standard deviation of less than 0.05Å. Since spectra were obtained in second order of a 1200 g/mm grating mounted in a 0.5 m double monochromator, the absolute energy uncertainties (three standard deviations) are expected not to exceed $\pm$ 0.3 cm^{-1}.

V. RESULTS AND DISCUSSION

The results of the 90° Raman scattering experiments are summarized in Table 1 and spectra of the neat crystals are shown in Figures 4 through 7. Mixed crystal experiments were attempted to obtain information about the crystal site symmetries. These experiments were not entirely successful. GeF_4 occupies several sites in SiF_4 and at higher concentrations a portion is excluded (deduced from variation of spectra along length of the crystal and occurrence of neat crystal peaks). SiF_4 on the contrary appears to occupy unique sites in GeF_4. (See Figures 8-10.) This behavior can be correlated with the fact that the Si-F bond length[17] (1.56Å) is less than the Ge-F bond length[1] (1.67Å) in the gas phase molecules. However, the situation is not so straightforward since the densities of SiF_4[4] at -170°C (2.18 g/cc) and of GeF_4[18] at -195°C (3.148 g/cc) yield values of packing densities of 1.23×10^{22} and 1.25×10^{22} molecules/cc. Apparently the larger number of electrons in Ge increases the Ge-Ge and Ge-F attraction requiring shorter F-F contacts to create balancing repulsive interactions. Unfortunately, however, even for the substituted SiF_4 in GeF_4 single crystals, weak signals necessitated the use of slit widths too large to yield useful ν_3 and ν_4 site information.

The neat crystal data are presented in Table 1. Their previous TO/LO splitting assignments for a cubic crystal are given therein for discussion convenience only. We have further observed the splitting of the ν_3 and ν_4 TO components in SiF_4 but not in GeF_4. The similarity of Raman spectra suggest that GeF_4 could have a more symmetrical structure than SiF_4. Assuming the deviation from T_d^3 is small, polariton behavior and the assumed TO/LO splittings can at least be tested for consistency based on molecular dipole properties. Figure 11 displays the values of $\left(\frac{\partial \mu}{\partial Q_i}\right)$ required by equation 1 to fit the observed crystal splittings.

For SiF_4 the agreement with the vapor phase values of the dipole derivatives seems adequate.[19] The increased mass of Ge may be cited for the decreased value of $\left(\frac{\partial \mu}{\partial Q_3}\right)$ (since the Q's are mass weighted normal coordinates). The relative constancy of $\left(\frac{\partial \mu}{\partial Q_4}\right)$ between the two systems may be due to small motion of the central atom in this mode.[20]

To test the hypothesis that these splittings are in fact due to dipolar TO/LO effects, small scattering angle experiments were performed on a thin disc shaped single crystal of SiF_4. A low power He-Ne laser was used to define the scattering direction and to test (with back reflections) for perpendicularity of surfaces. Mirrors on adjustable mounts were used to direct the unfocused incident Ar^+ laser beam into the sample. Again assuming perfect T_d^3 SiF_4 symmetry, dispersion curves were calculated for reasonable values (unmeasured) of ε_∞ and the observed 90° spectra. These, together with the phase matching requirements for various angles, are presented in Figure 1. Raman scattering at a particular angle is allowed at the intersection of a dispersion curve and the appropriate phase matching curve. Scattering angles (in the crystal) between 0 and 4.5 $(\varepsilon_\infty)^{-\frac{1}{2}}$ degrees were investigated. While observation of polariton dispersion in the ν_4 branch may be beyond the experimental capacity, the behavior of the largely ν_3 polariton (TO) branch should have been quite dramatic. No peaks were observed at energies differing by more than 0.3 cm^{-1} from the 90° scattering spectra. The curves predict a deviation of at least 40 cm^{-1} for angles less than 4° (in vacuum exterior to the crystal).

It was necessary to enhance the 0° spectra on a signal averager due to the requisite small scattering solid angle. After ten to twenty scans, the spectra were integrated and intensities of the various peaks tabulated and normalized to the ν_1 peak intensity. The "TO" to "LO" branch intensity ratio

remained constant to within roughly 20%. The absence of any angle-dependent intensity (or in general any increase in the baseline) at lower energy than the 90° ν_3 peaks is at variance with the polariton model. Even if there were destructive interference between the three-wave mixing and true Raman mechanisms, a complete cancellation could occur only at one angle; that is, only for one ratio of photon to phonon admixture coefficients. However, at the "knees" of the dispersion curves, both the energies and the admixture are changing rapidly. This fact, coupled with the earlier discussion of scattering geometry and approximate selection rules, suggests that the magnitude of the scattering matrix element is not responsible for failure to observe lower energy intensity.

One difficulty with the present experimental situation for these systems is the discrepancy in magnitudes of splitting within the ν_3 and ν_4 TO branches between our data and those of Bessette et al.[7] Our Raman spectra were obtained using large vapor grown single crystals while reference 7 indicates the use of polycrystalline melt grown samples. One might initially attempt to dismiss this difference (Table 1) as merely an angular phenomenon as is indicated in Figure 3. Bessette et al. suggest crystal structures with C_3^4 or C_{3v}^5 as possible space groups. For uniaxial crystals with small differences in frequencies of vibrations (of an isolated band) parallel and perpendicular to the uniaxis, $\hat{c}$, the frequencies of the extraordinary mode of the TO branch satisfies[11]

$$\omega^2 \approx \omega_{\parallel}^2 \sin^2\phi + \omega_{\perp}^2 \cos^2\phi$$

when $\underline{k}$ is inclined at an angle ϕ to $\hat{c}$. Our values of the would-be TO splittings for ν_4 and ν_3, 0.5 and 3.4 cm^{-1}, and the values of Bessette et al., 2.7 and 3.5 cm^{-1}, do not fit into the approximate form

$$\omega - \omega_{\perp} \approx \frac{1}{2}\left(\frac{\omega_{\parallel}^2 - \omega_{\perp}^2}{\omega_{\perp}}\right) \sin^2\phi .$$

Moreover, the frequencies of the ordinary (lower energy) branch, $\omega_\perp$, should be equal. While there is some indication of calibration differences (in ν_1 and ν_2), the large differences in ν_4 TO are beyond this. It may be possible to attribute these differences to crystal size or temperature effects. They are, however, clearly not associated with polariton phenomena.

It is necessary to consider alternative explanations of the data since predicted TO-polariton model behavior (e.g., intensity and position variation of scattering peaks with scattering angle Θ) has not been observed. The existence in general of polaritons in inorganic (ionic) crystals seems well documented[15,21-23], and therefore one must consider alternatives for which the splittings derive from another source (i.e., site and/or Davydov splitting). Magnitude of polariton coupling must then be reduced due to the different unit cell mechanical vibrations created. The analysis of all possible structures consistent with such an interpretation is not a reasonable approach to this problem since spectra need not in general exhibit all group theoretically predicted features.

We must, however, consider the other evidence for TO/LO splittings and demonstrate that it is also consistent with site and Davydov splittings in a possibly non-cubic multimolecule per unit cell crystal. First, observation of one of the components of both the ν_3 and ν_4 structures in Raman scattering but not in infrared absorption may be a simple selection rule phenomenon (not necessarily of the g/u type). Second, observation of reflection spectra bracketed by the $\underline{k} \sim 0$ components is expected for (intense) dipole bands with $\underline{k} = 0$ components at the top and bottom of the bands. Third, the approximate agreement of splittings characteristic of a TO/LO model with those calculated from the squares of dipole derivative is not unique. The Davydov splittings would also depend on these parameters through lattice sums. On the other hand, polariton behavior would be lessened because of the increased number of unit cell vibrations coupling to

the electromagnetic field; photon-phonon coupling is through translationally equivalent entities (unit cells). It is the unit cell dipole moment that couples to the radiation field.

As to the agreement of transition dipole calculations with observed two-particle structure found in the infrared for $\nu_1 + \nu_3$, $\nu_1 + \nu_4$, and $\nu_2 + \nu_3$, we would suggest that it is the approximate molecular density (spacing of molecules) which determines the overall density of states. The fact that a threefold degenerate vibration is involved means that if smaller site and unit cell anisotropies are ignored, the direction of the molecular dipole is not uniquely determined. In this regard, the similarities between the SiF_4 $\nu_1 + \nu_3$, $\nu_2 + \nu_3$, and $\nu_1 + \nu_4$ two-particle spectra[8] and the UF_6 $\nu_1 + \nu_3$ and $\nu_2 + \nu_3$ two-particle spectra are particularly striking and revealing.[24,25] The UF_6 single-particle spectra are characterized by site splittings and large exciton splittings, which derive from four inequivalent molecules in the unit cell. Nonetheless, the apparent differences (perhaps selection-rule related) between the SiF_4 and UF_6 single-particle spectra notwithstanding, the SiF_4 and UF_6 two-particle spectra are practically identical. This, of course, implies that the density of states for the dipolar levels (ν_3 and ν_4) are very similar in these cases.[25] Furthermore, gerade $\underline{k} = 0$ components have been observed <u>throughout</u> the UF_6 ν_3 fundamental band region, removing any simple identification of the bimodal distribution of states with transverse or longitudinal character.

Finally, it is appropriate to emphasize that detailed polarization data, while of course interesting and ultimately useful, would be of little help for the further resolution of the exciton vs. TO/LO ν_3 and ν_4 splitting mechanisms. The reasons for this are obvious: an accurate structure determination does not exist at present and the exact polarization data for resolved peaks is completely dependent on unit cell and space group specifics;

crystal growth direction is apparently random and polarized light techniques could not readily locate special directions; polarizations are not unique to LO and polariton-TO modes but are present for exciton components as well; and ν_3 and ν_4 polarizations can be mixed for a given spectral feature due to unresolved $\underline{k} = 0$ exciton structure in accord with the above assignments. Therefore, the only unique feature of the polariton model appears to be angular dependence of peak intensities and energies: no such dependence has been observed in the Raman scattering of SiF_4 or GeF_4.

VI. CONCLUSIONS

We would add our suggestion to that of Bessette et al. that the crystal structure of SiF_4 (GeF_4) be reinvestigated. There are several ambiguities in the vibrational spectra which could be resolved if the structures were actually known. Moreover careful polarization studies on orientated single crystals would then be worthwhile.

The LO/TO-polariton model for the ν_3 and ν_4 vibrations is not successful in explaining the observed Raman spectra of SiF_4 (GeF_4) even if the crystal structures are allowed to be arbitrarily uniaxial with one molecule per primitive unit cell. The main unique feature of this model is a scattering angle dependent spectrum which is not substantiated in 0° and 90° Raman scattering.

The Raman scattering spectrum of GeF_4 is somewhat simpler than that of SiF_4. "Splitting" of the low energy components of ν_3 and ν_4 has not been observed. Apparently the crystal structure of GeF_4 is closer to an ideal high symmetry space group than SiF_4.

The failure of GeF_4 to occupy simple unique (substitutional) sites in SiF_4 is observed, as is the apparent exclusion of GeF_4 at moderate concentrations, even though the neat crystals have nearly equal molecular packing densities. A detailed study of the structure and interactions in these molecular crystals seems warranted.

We would suggest that the observed splittings previously assigned as transverse and longitudinal components are in fact Davydov components of dipolar exciton bands. The polariton dispersion curves in this case would be drastically altered; the electromagnetic field vibrations must couple with unit cell mechanical vibrations. This would alter the expectations for possible angle dependent Raman spectra.

REFERENCES

1. A. D. Caunt, L. N. Short and L. A. Woodward, Trans. Far. Soc., 48, 873 (1952); O. Linnett and V. Heath, J. Chem. Phys., 19, 801 (1951).

2. M. Atoji and W. N. Lipscomb, Acta Crys., 7, 597 (1954).

3. J. W. Stewart, J. Chem. Phys., 33, 128 (1960).

4. E. L. Pace and J. S. Mosser, J. Chem. Phys., 39, 154 (1963).

5. R. M. Hexter, J. Chem. Phys., 37, 1347 (1962).

6. D. Fox and R. M. Hexter, J. Chem. Phys., 41, 1125 (1964).

7. F. Bessette, A. Cabana, R. P. Fournier and R. Savoie, Can. J. Chem., 48, 410 (1970).

8. U. Schettino, Chem. Phys. Lett., 18, 535 (1973).

9. D. P. Craig and U. Schettino, Chem. Phys. Lett., 23, 315 (1973).

10. G. Turrell,"Infrared and Raman Spectra of Crystals"(Academic Press, New York, 1972); and M. M. Sushchinskii,"Raman Spectra of Molecules and Crystals"(Keter, Inc., New York, 1972).

11. R. Loudon, Adv. Phys., 13, 423 (1964); A. S. Barker and R. Loudon Rev. Mod. Phys., 44, 18 (1972); and C. Y. She, J. D. Masso and D. F. Edwards, J. Phys. Chem. Solids, 32, 1887 (1971).

12. R. Loudon, in"Light Scattering Spectra of Solids", Ed. by G. B. Wright (Springer-Verlag, New York, 1969),page 25.

13. E. Burstein, S. Ushioda, A. Pinczuk and J. F. Scott, in "Light Scattering Spectra of Solids", Ed. by G. B. Wright (Srpinger-Verlag, New York, 1969), page 4.

14. W. Vedder and D. F. Hornig, Adv. Spec., 2, 189 (1961).

15. C. H. Henry and J. J. Hopfield, Phys. Rev. Lett., 15, 964 (1965).

16. G. R. Meredith Thesis, Princeton University, 1976.

17. B. Beagley, D. P. Brown and J. M. Freeman, J. Mol. Structure, 18, 337 (1973).

18. Research Inorganic Chemicals, Product information.

19. P. N. Schatz and D. F. Hornig, J. Chem. Phys., 21, 1516 (1953).

20. G. Herzberg, "Molecular Spectra and Molecular Structure II. Infrared and Raman Spectra of Polyatomic Molecules", (Van Nostrand Reinhold Co., New York, 1945), page 100.

21. S. P. S. Porto, B. Tell and T. C. Damen, Phys. Rev. Lett., 16, 450 (1966)

22. J. F. Scott and S. Ushioda, in "Light Scattering Spectra of Solids," Ed. by G. B. Wright (Springer-Verlag, New York, 1969), page 57.

23. G. G. Mitin, V. S. Gorelik, L. A. Kulenskii, Yu. N. Polivanov, and M. M. Sushcinskii, Zh. Eksp. Teor. Fiz. 68, 1757 (1975); [English Translation: Sov. Phys. JETP 41, 882 (1976)].

24. R. Bougon and P. Rigny, C. R. Acad. Sci. Paris, C 263, 1321 (1966).

25. E. R. Bernstein and G. R. Meredith, to be published (Chem. Phys.).

Table 1. Summary of Crystal Spectra.

	FREQUENCIES (cm^{-1})					ASSIGNMENT[a]	
	INFRARED		RAMAN				
	Bessette, et al.[b]	Schettino[c]	Bessette, et al.	Schettino	This Work[d]		
A. SiF_4			258.3	261	259.0 (.4)	ν_2	
	370.3	374	370.6	374	373.5 (1.2)	ν_4	(Transverse)
	373.7		373.3		374.0		
			407.5	410	408.3 (.8)		(Longitudinal)
	795		795.3	797	796.2 (.9)	ν_1	
	987.7		987.8		988.2 (2.2)	ν_3	(Transverse)
	991.2	992	991.3	991	991.6 (1.8)		
			1057.3	1058	1058.3 (1.1)		(Longitudinal)
B. GeF_4					194.8 (1.0)	ν_2	
					253.2 (.9)	ν_4	(Transverse)
					301.8 (1.0)		(Longitudinal)
					729.5 (<.3)	ν_1	
					774.4 (.8)	ν_3	(Transverse)
					817.9 (.6)		(Longitudinal)

a. Old (SiF_4) TO/LO ν_3-ν_4 assignments and parallel ones in GeF_4 are indicated in parentheses for discussion purposes only (see text).

b. Reference 7.

c. Reference 8.

d. Measured FWHH are listed in parentheses.

Figure 1. Polariton Dispersion Curves for SiF_4. Based on equation 1 of section III and the observed (90°) frequencies, dispersion curves were calculated for a range of values of the infinite frequency (optical) dielectric constant. The phonon modes are pure and are triply degenerate at $\underline{k} = 0$. At small finite waves the longitudinal modes appear at constant frequency. The transverse modes mix with the transverse electromagnetic field causing the anticrossing behavior shown. These transverse modes are doubly degenerate.

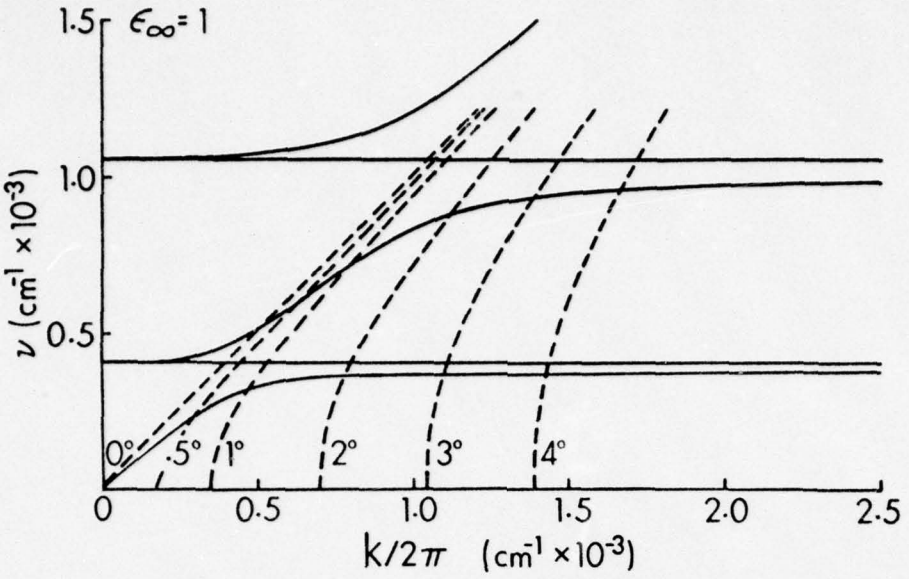
$\epsilon_\infty = 1$
ν (cm^{-1} × 10^{-3})
1.5
1.0
0.5
0°
.5°
1°
2°
3°
4°
0
0.5
1.0
1.5
2.0
2.5
$k/2\pi$ (cm^{-1} × 10^{-3})

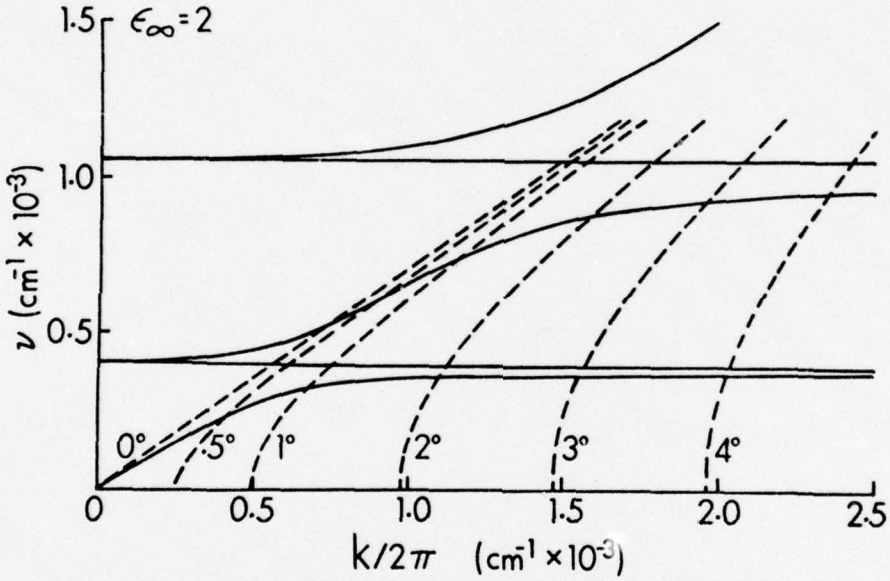
$\epsilon_\infty = 2$
ν (cm^{-1} × 10^{-3})
1.5
1.0
0.5
0°
.5°
1°
2°
3°
4°
0
0.5
1.0
1.5
2.0
2.5
$k/2\pi$ (cm^{-1} × 10^{-3})

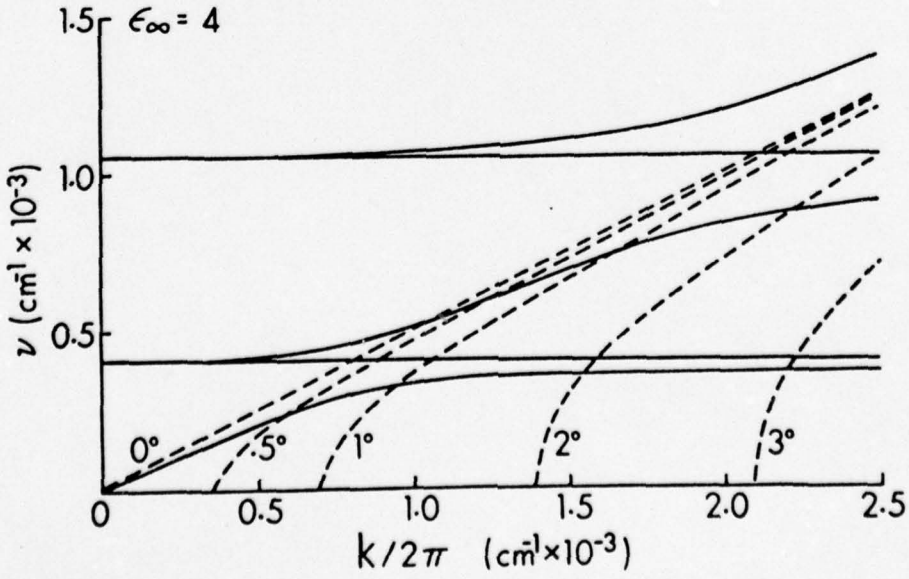
$\epsilon_\infty = 4$
ν (cm^{-1} × 10^{-3})
1.5
1.0
0.5
0°
.5°
1°
2°
3°
0
0.5
1.0
1.5
2.0
2.5
$k/2\pi$ (cm^{-1} × 10^{-3})

Figure 2. Geometry of Raman scattering as depicted in the inset; $\underline{k}_i$ is the incident photon wavevector, $\underline{k}_s$ is the scattered photon wavevector, $\underline{k}$ is the (crystal) wavevector of the created excitation, and Θ is the scattering angle. The variation of relative orientation of $\underline{k}$ to $\underline{k}_i$ (equation 6) is shown for small scattering angles and various polariton frequencies. Curves A through G represent polariton frequencies ν = 0 cm^{-1} (A) through ν = 1200 cm^{-1} (G) in increments of 200 cm^{-1}.

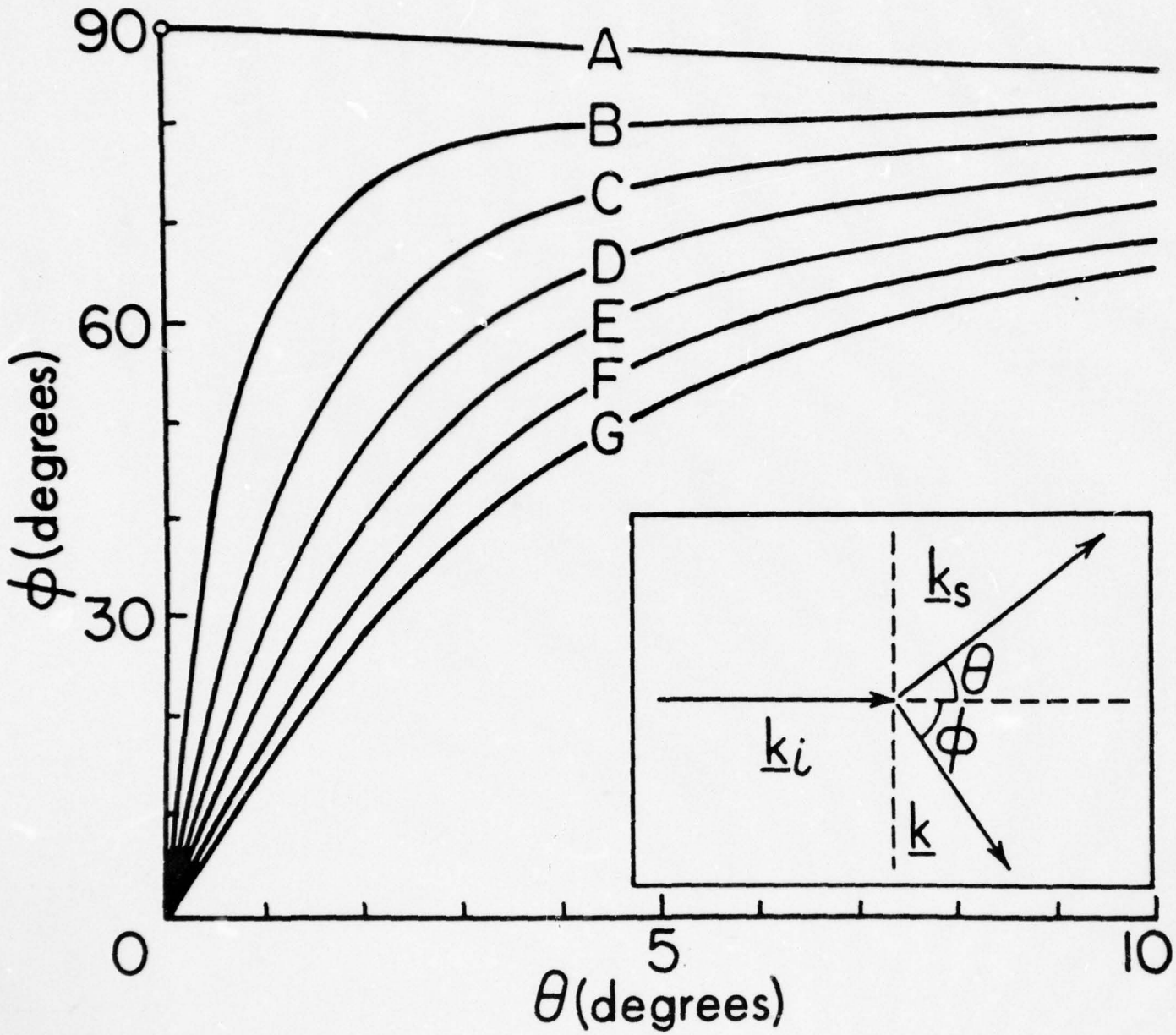
90
60
30
0
5
10
A
B
C
D
E
F
G
φ(degrees)
θ(degrees)
k_s
θ
k_i
φ
k

Figure 3. Polariton Dispersion Curve for Uniaxial Crystal (from reference 11). At zero wavevector there are two degenerate modes polarized perpendicular to the uniaxis and one nondegenerate mode polarized along the uniaxis. For wavevector parallel to the uniaxis the perpendicular modes couple to the electromagnetic field and remain degenerate as shown in a. For wavevector perpendicular to the uniaxis one of the perpendicular modes and the parallel mode couple with the field to become transverse modes, the parallel mode creating an extraordinary mode with higher frequency as shown in c. For arbitrary wavevector inclination a general mixing occurs to create the transverse and longitudinal modes as shown in b.

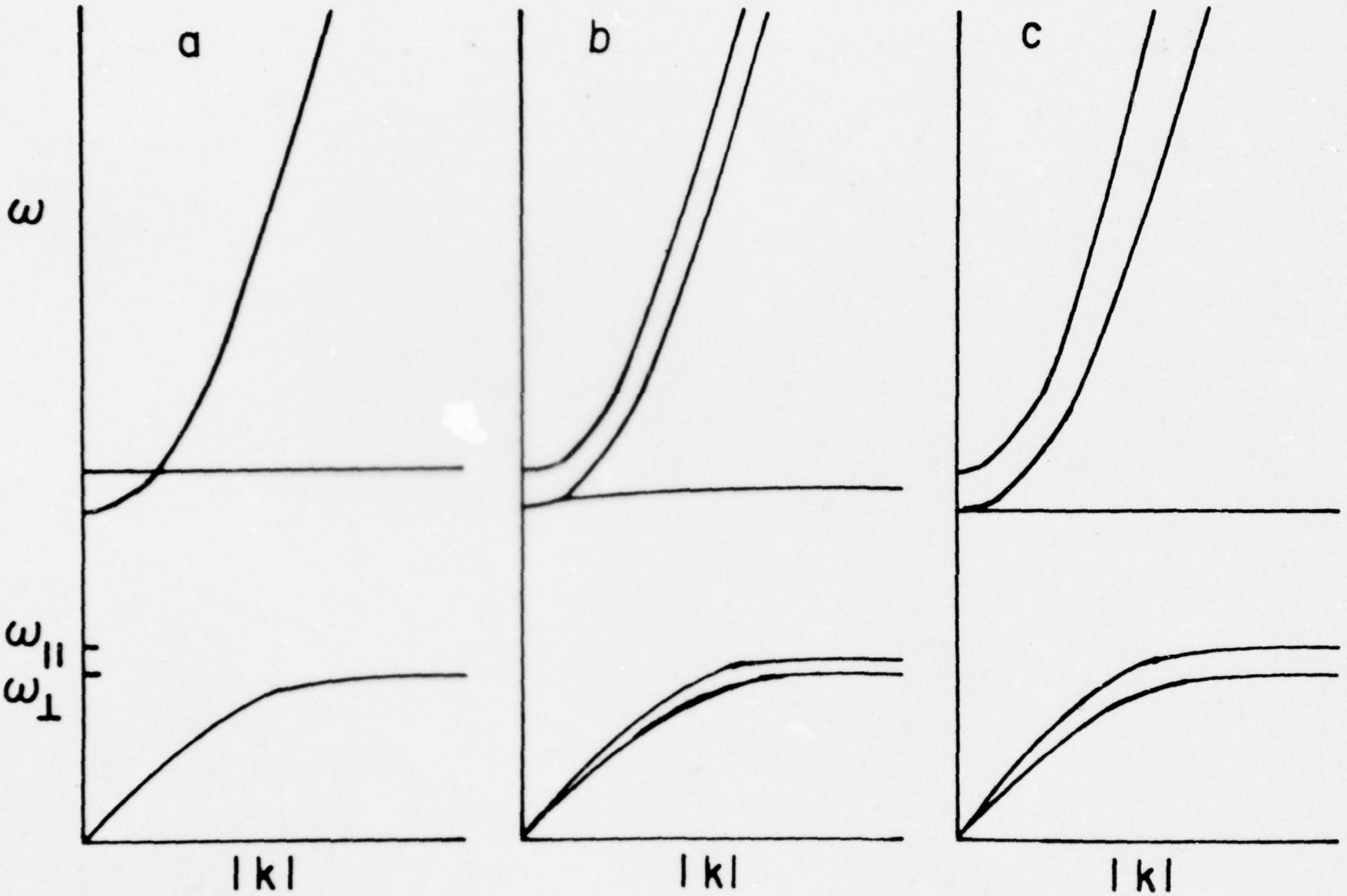
a
b
c
ω
ω∥
ω⊥
|k|
|k|
|k|

Figure 4. 90° Raman Spectra of ν_1 Regions.

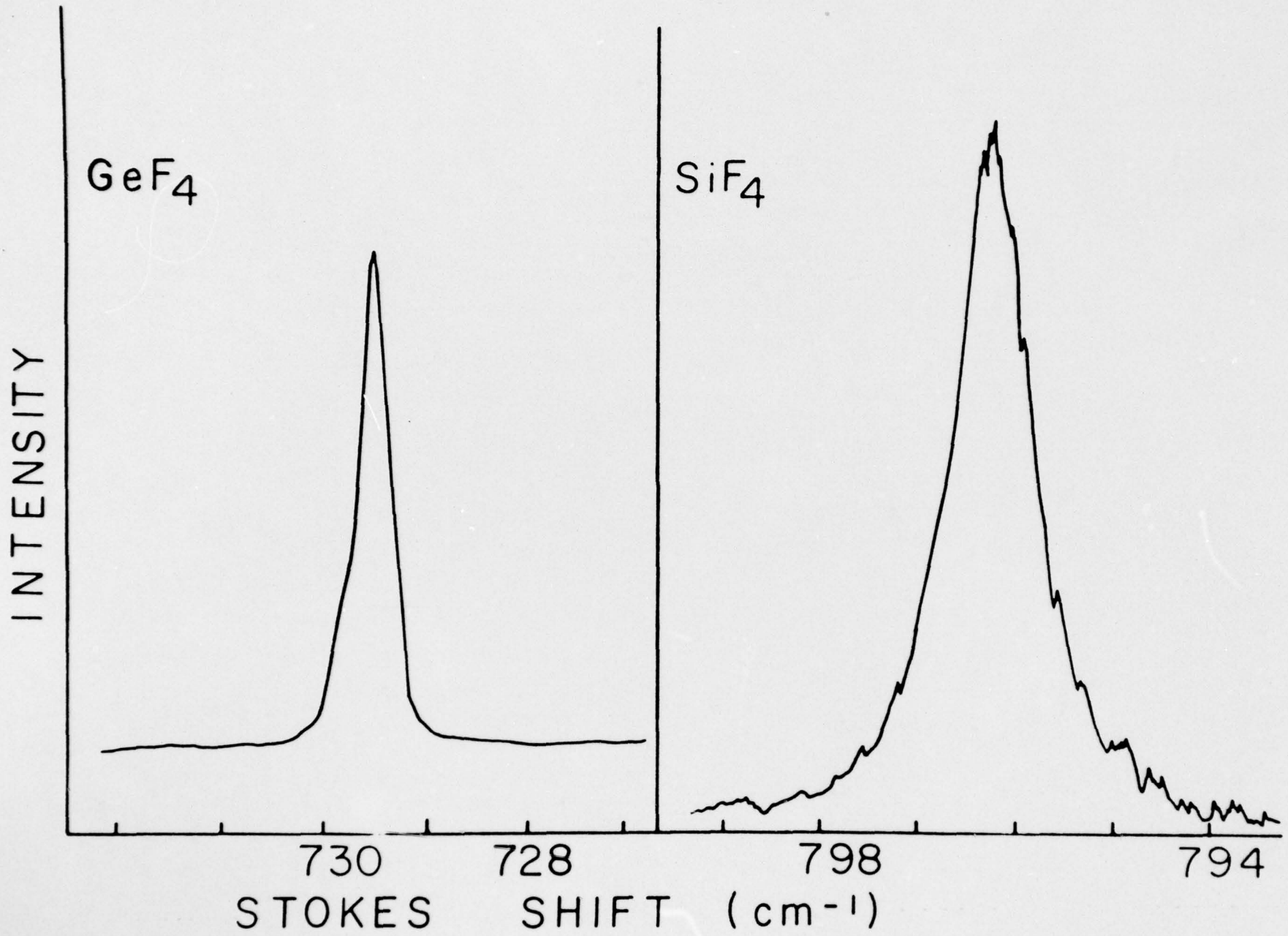
GeF4
SiF4
INTENSITY
730
728
798
794
STOKES SHIFT (cm-1)

Figure 5. 90° Raman Spectra of ν_2 Regions.

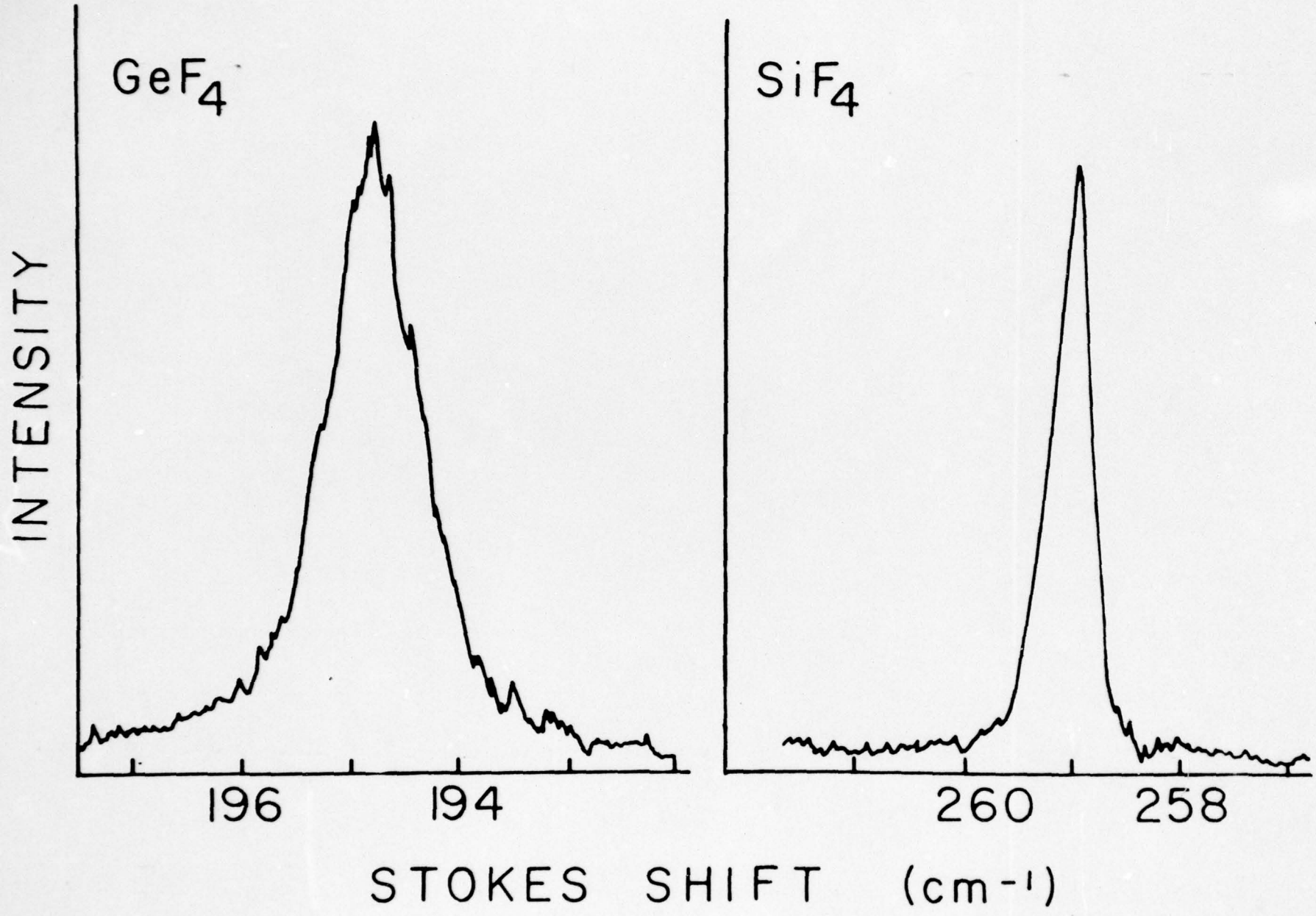
GeF4
SiF4
INTENSITY
196
194
260
258
STOKES SHIFT (cm-1)

Figure 6. 90° Raman Spectra of the SiF_4 and GeF_4 ν_3 Region.

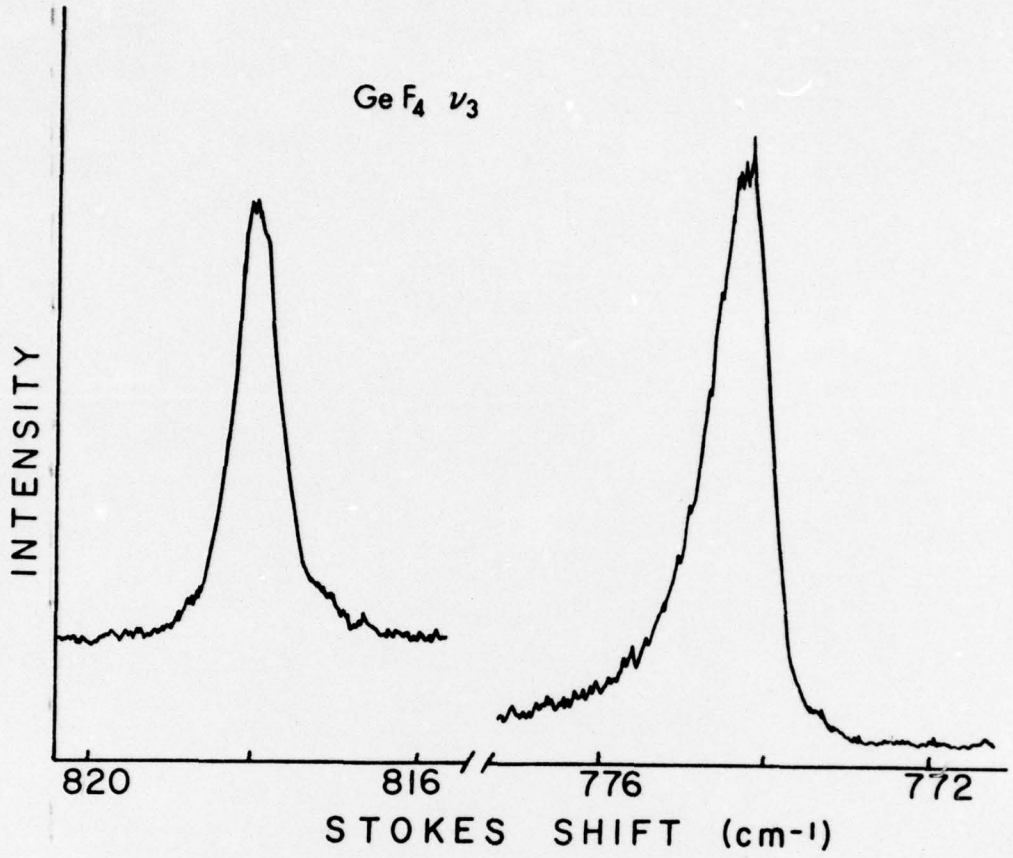
Ge F4 ν3
INTENSITY
820
816
776
772
STOKES SHIFT (cm-1)

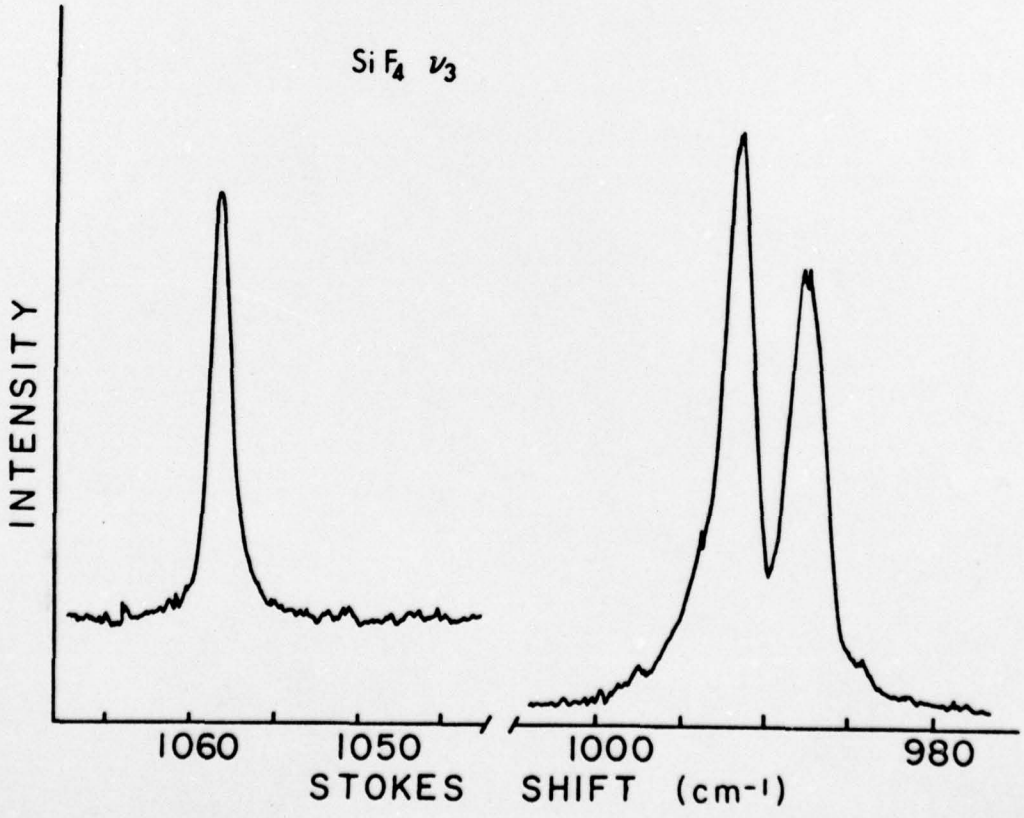
Si F4 ν3
INTENSITY
1060
1050
1000
980
STOKES SHIFT (cm-1)

Figure 7. 90° Raman Spectra of the SiF_4 and GeF_4 ν_4 Region.

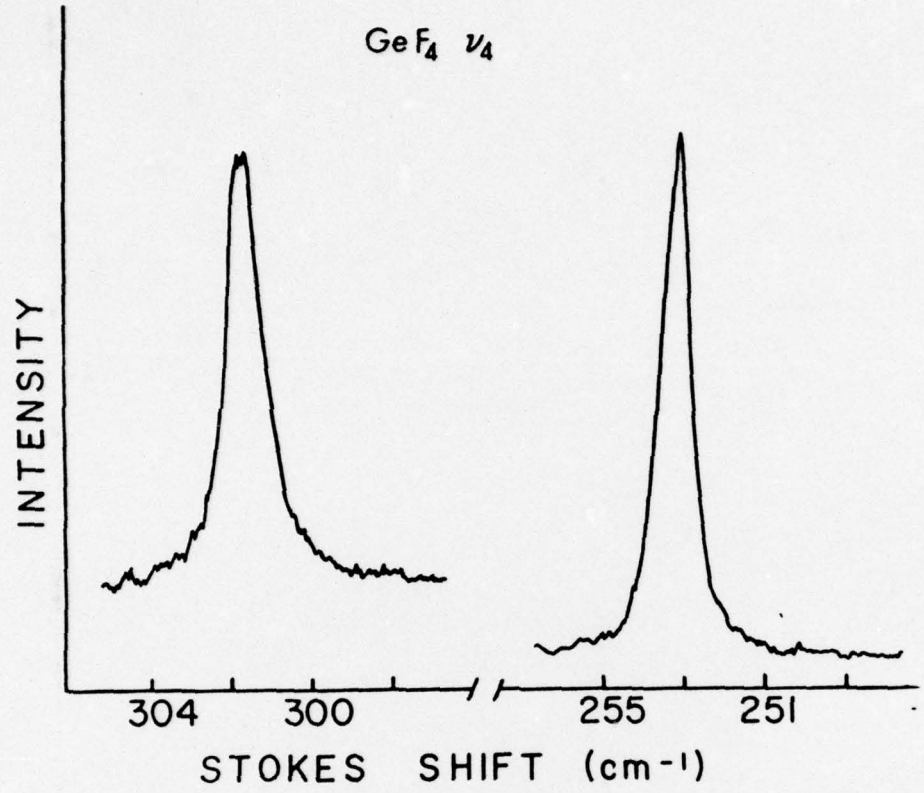
GeF4 ν4
INTENSITY
304
300
255
251
STOKES SHIFT (cm-1)

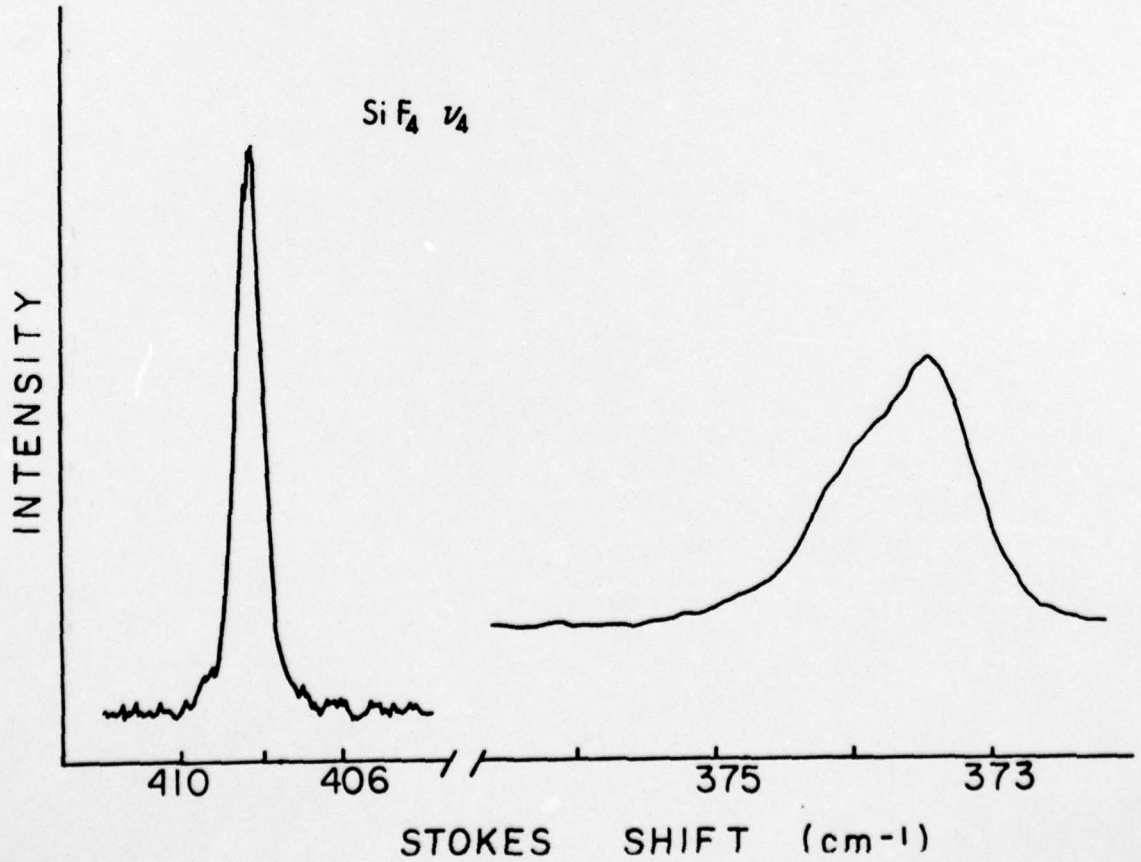
SiF4 ν4
INTENSITY
410
406
375
373
STOKES SHIFT (cm-1)

Figure 8. 90° Raman Spectrum of the ν_1 Region of GeF_4 in a Nominal 5% GeF_4 in SiF_4 crystal. The multiplicity of peaks indicates several sites. The peak near 730 cm^{-1} corresponds to the neat crystal vibrational transition. The relative intensities of these peaks were observed to vary depending on the particular portion of crystal examined.

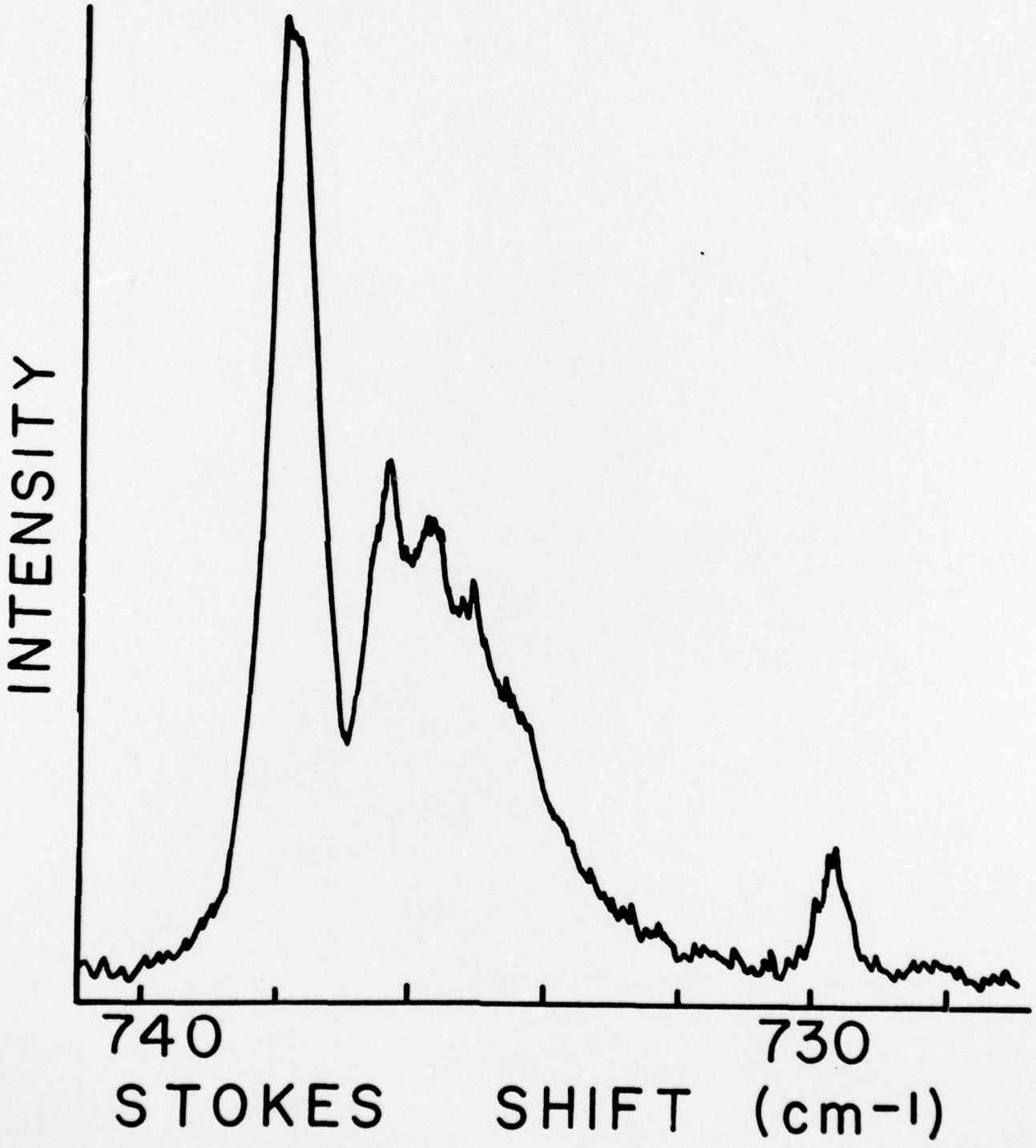
INTENSITY
740
730
STOKES SHIFT (cm-1)

Figure 9. 90° Raman Spectrum of the ν_2 Region of GeF_4 in a Nominal 5% GeF_4 in SiF_4 Crystal. Comments given in the caption of Figure 8 are applicable here. The neat crystal transition is also observed near 195 cm^{-1}. The similarity of this structure to that of Figure 8 should be noted.

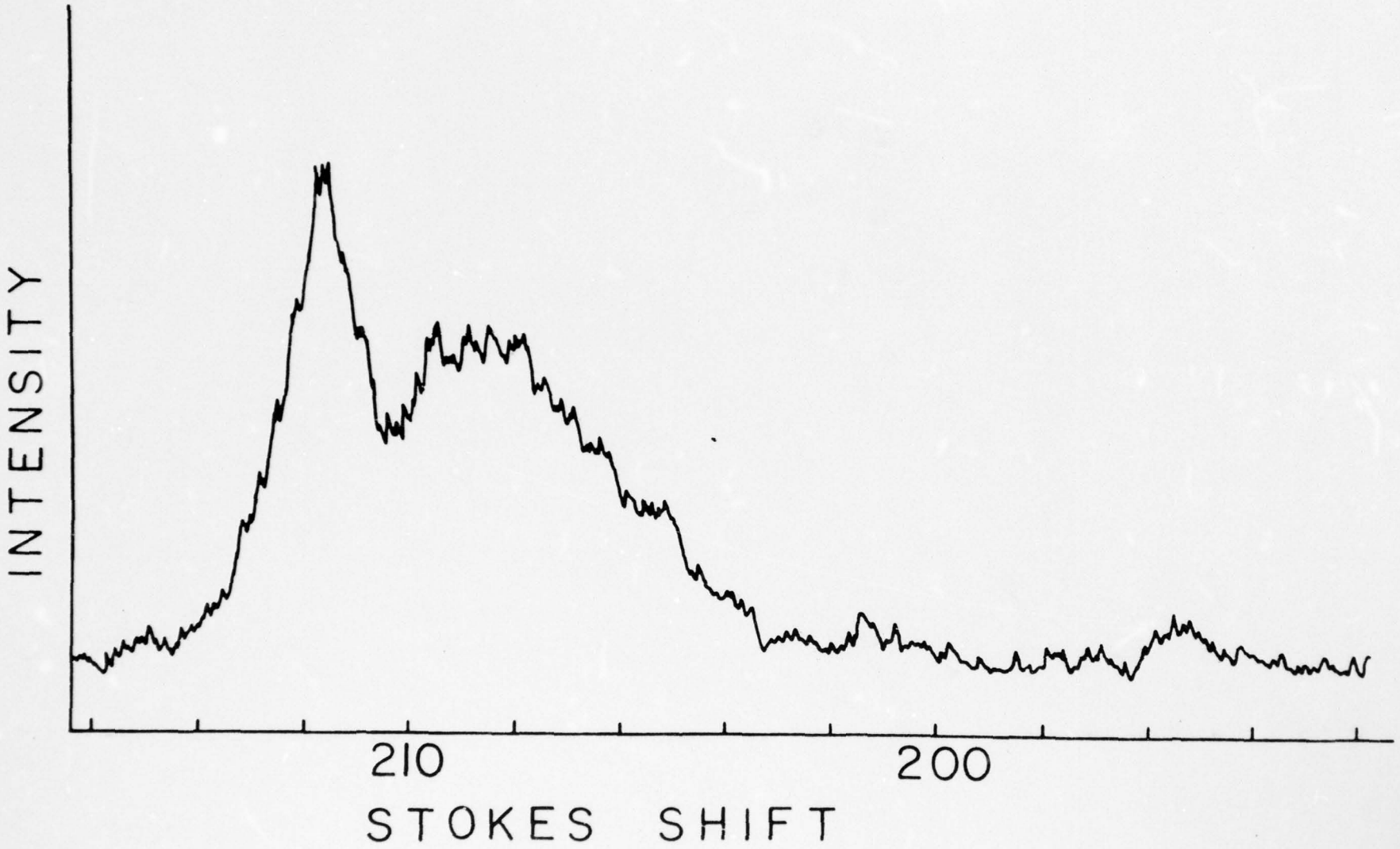
INTENSITY
210
200
STOKES SHIFT

Figure 10. 90° Raman Spectrum of the ν_1 Region of SiF_4 in a Nominal 5% SiF_4 in GeF_4 Crystal. The slight upward shift (~0.4 cm^{-1}) and single peak are indications that the SiF_4 occupies substitutional sites in the GeF_4 structure.

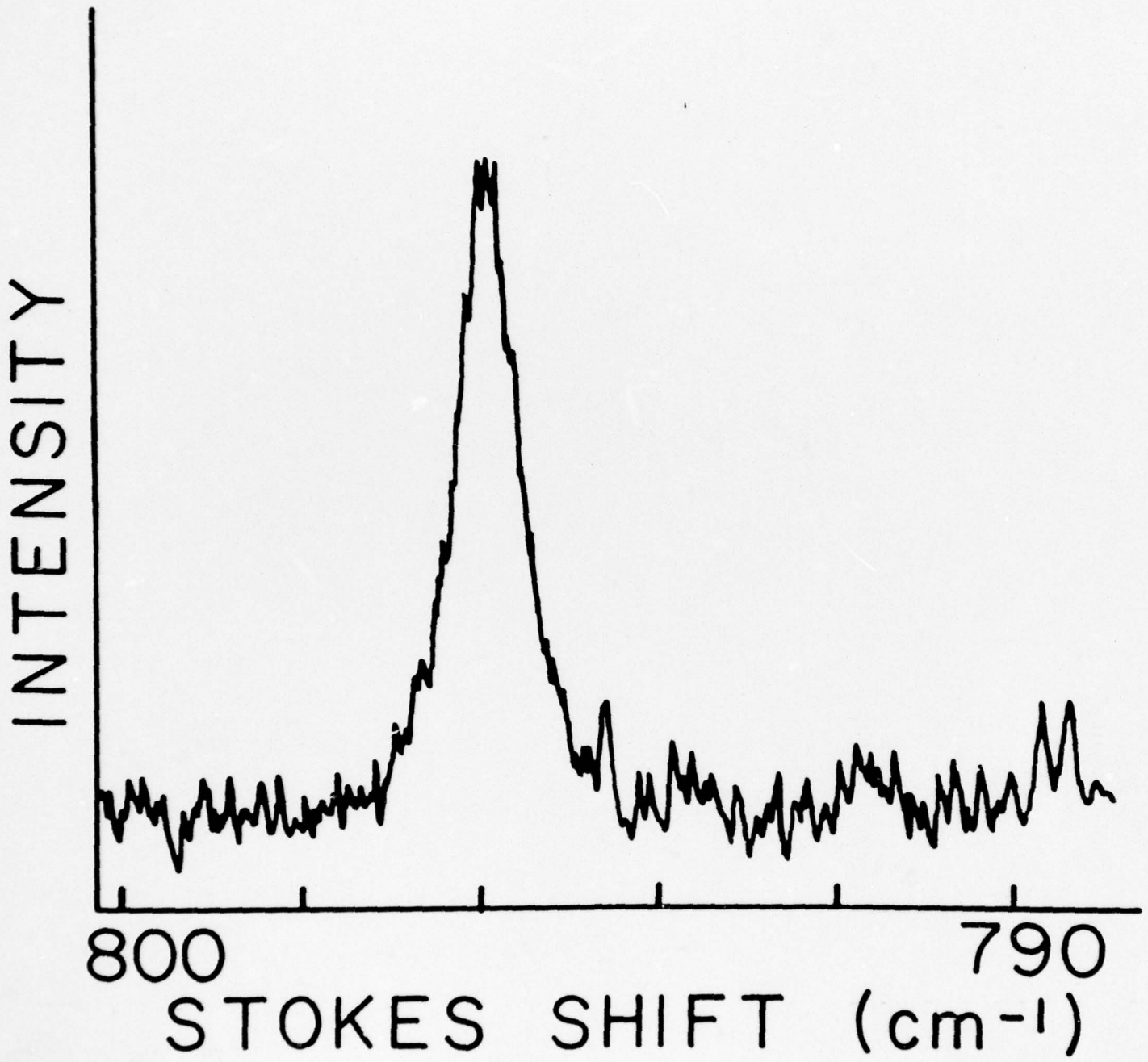
INTENSITY
800
790
STOKES SHIFT (cm-1)

Figure 11. Molecular Electric Dipole Derivatives. The calculated values are derived from equation 1 to fit the 90° spectra as a function of ε_∞ . Only the magnitude and not the sign of the derivatives are known here.

A) Value for the ν_3 mode of SiF_4

B) Value measured for the ν_3 mode of SiF_4 in vapor phase (ref. 18)

C) Value for the ν_3 mode of GeF_4

D) Value for the ν_4 mode of SiF_4

E) Value for the ν_4 mode of GeF_4

F) Value measured for the ν_4 mode of SiF_4 in vapor phase (ref. 18)

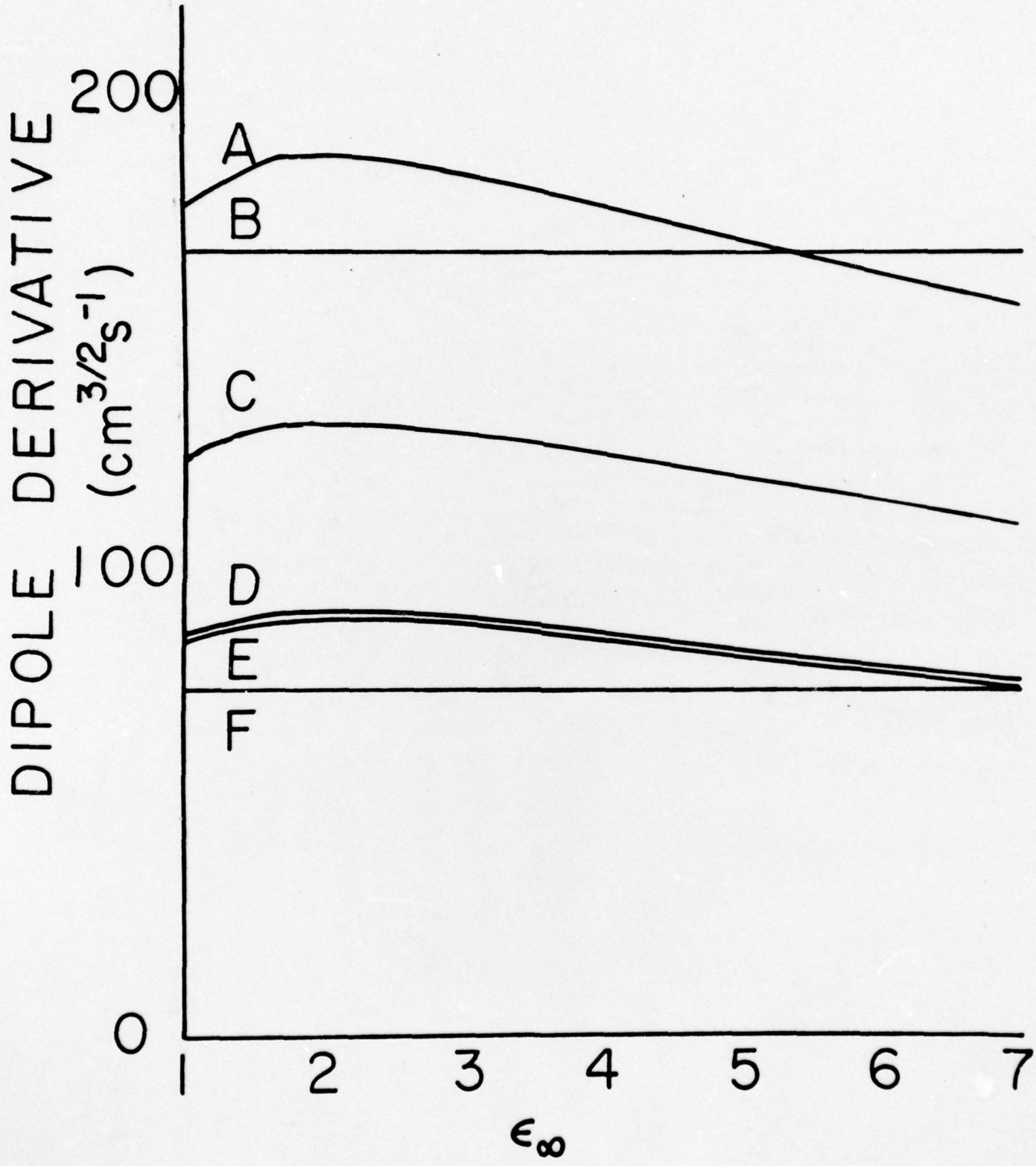
DIPOLE DERIVATIVE
(cm^3/2 s^-1)
200
100
0
A
B
C
D
E
F
1
2
3
4
5
6
7
ε∞